HEPATOLOGY

HEPATOLOGY, VOL. 73, NO. 2, 2021

TMEM9-v-ATPase Activates Wnt/β-Catenin Signaling Via APC Lysosomal Degradation for Liver Regeneration and Tumorigenesis

Youn-Sang Jung,[1,2] Sabrina A. Stratton,[3] Sung Ho Lee,[1] Moon-Jong Kim,[1] Sohee Jun,[1] Jie Zhang,[1] Biyun Zheng,[1] Christopher L. Cervantes,[1] Jong-Ho Cha,[4] Michelle C. Barton,[3,5] and Jae-Il Park[1,5,6]

BACKGROUND AND AIMS: How Wnt signaling is orchestrated in liver regeneration and tumorigenesis remains elusive. Recently, we identified transmembrane protein 9 (TMEM9) as a Wnt signaling amplifier.

APPROACH AND RESULTS: TMEM9 facilitates v-ATPase assembly for vesicular acidification and lysosomal protein degradation. TMEM9 is highly expressed in regenerating liver and hepatocellular carcinoma (HCC) cells. TMEM9 expression is enriched in the hepatocytes around the central vein and acutely induced by injury. In mice, *Tmem9* knockout impairs hepatic regeneration with aberrantly increased adenomatosis polyposis coli (Apc) and reduced Wnt signaling. Mechanistically, TMEM9 down-regulates APC through lysosomal protein degradation through v-ATPase. In HCC, TMEM9 is overexpressed and necessary to maintain β-catenin hyperactivation. TMEM9–up-regulated APC binds to and inhibits nuclear translocation of β-catenin, independent of HCC-associated β-catenin mutations. Pharmacological blockade of TMEM9-v-ATPase or lysosomal degradation suppresses Wnt/β-catenin through APC stabilization and β-catenin cytosolic retention.

CONCLUSIONS: Our results reveal that TMEM9 hyperactivates Wnt signaling for liver regeneration and tumorigenesis through lysosomal degradation of APC. (Hepatology 2021;73:776-794).

Wnt signaling orchestrates multiple cellular processes such as cell proliferation, differentiation, adhesion, and migration during embryogenesis, organogenesis, tissue homeostasis, and regeneration.[1-4] β-catenin acts as a critical player in Wnt/β-catenin signaling. The β-catenin destruction complex, including adenomatosis polyposis coli (APC), casein kinase 1 (CK1), glycogen synthase kinase 3α/β (GSK3α/β), and AXIN, negatively controls β-catenin, which induces β-catenin proteolysis.[5] However, excessive activation of β-catenin induces hyperproliferation, leading to cancer.

Liver tissue shows a high capacity for regeneration when injured,[3] and Wnt/β-catenin signaling has been

Abbreviations: APC, adenomatosis polyposis coli; BAF, bafilomycin; cDNA, complementary DNA; ChIP, chromatin immunoprecipitation; CK1, casein kinase 1; CTB, cathepsin B; CV, central vein; DAPI, 4',6-diamidino-2-phenylindole; dpi, days post-inoculation; EDTA, ethylene diamine tetraacetic acid; Gs, glutamine synthetase; GSK3, glycogen synthase kinase 3; HCC, hepatocellular carcinoma; HNF4α, hepatocyte nuclear factor 4α; IB, immunoblot; IF, immunofluorescence; IHC, immunohistochemistry; KO, knockout; MVB, multivesicular body; PHx, partial hepatectomy; PLA, proximity ligation assay; RT-PCR, reverse-transcription PCR; SDS, sodium dodecyl sulfate; shRNA, short hairpin RNA; shTMEM9, short hairpin TMEM9; TBX3, T-box 3; TMEM9, transmembrane protein 9; Tris, trishydroxymethylaminomethane; WT, wild-type.

Received August 30, 2019; accepted April 8, 2020.

Additional Supporting Information may be found at onlinelibrary.wiley.com/doi/10.1002/hep.31305/suppinfo.

Supported by grants to the Cancer Prevention and Research Institute of Texas (RP140563 and RP200315 to J.-I.P.), the National Institutes of Health (R01 CA193297-01 to J.-I.P.), the Department of Defense Peer Reviewed Cancer Research Program (CA140572 to J.-I.P.), an Institutional Research Grant (MD Anderson Cancer Center to J.-I.P.), and SPORE in endometrial cancer (P50 CA83639 to J.-I.P.). The core facility (DNA sequencing and Genetically Engineered Moue Facility) was supported by the National Cancer Institute Comprehensive Cancer Center Grant to MD Anderson Cancer Center (P30 CA016672).

View this article online at wileyonlinelibrary.com.

DOI 10.1002/hep.31305

Potential conflict of interest: Nothing to report.

shown to play crucial roles in liver regeneration.[6-9] T-box 3 (*Tbx3*) and *Axin2*, a Wnt/β-catenin target gene, are highly expressed in liver lobules around the central vein (CV) during homeostatic renewal and regeneration.[10-12] In the setting of liver injury, these cells show high cell proliferative capacity through Wnt/β-catenin target genes such as cyclin D1.[3] Consistently, it has been shown that β-catenin contributes to hepatocyte proliferation[9] and growth.[13,14] Conversely, liver-specific β-catenin/*Ctnnb1* knockout (KO) mice exhibit reduced liver size with decreased hepatocyte proliferation[9] and impaired liver regeneration.[9] Despite such relevance of Wnt/β-catenin to liver regeneration, it remains elusive how Wnt/β-catenin signaling is activated following liver injury.

The aberrant activation of the Wnt/β-catenin signaling is directly associated with HCC. HCC shows frequent genetic mutations in β-catenin/*CTNNB1* (11%-37% of patients), *AXIN* (5%-15%), or *APC* (1%-2%) genes in HCC.[15,16] β-catenin/*CTNNB1* mutation allows β-catenin to escape an inhibitory function of the APC complex, resulting in hyperactivation of Wnt signaling.[17] Despite the pivotal roles of genetic mutations in the core components of the Wnt pathway, accumulating evidence suggests that additional layers of Wnt signaling regulation are deregulated and contribute to β-catenin target gene activation and tumorigenesis.[18-20] For instance, secreted Wnt ligands or agonists further enhance β-catenin target gene transactivation.[21,22] Additionally, mutated APC still negatively modulates β-catenin.[22] Building on these findings, we recently revealed that deregulated v-ATPase, a vacuolar proton pump, amplifies Wnt signaling in colorectal cancer.[23] Therefore, it is highly likely that beyond the core components of Wnt/β-catenin signaling, further layers of Wnt signaling regulation might contribute to hepatic tumorigenesis.

TMEM9 is a type I transmembrane protein that is localized primarily in the lysosomes and the late endosomes, also called the multivesicular bodies (MVBs).[24] Previously, we discovered that TMEM9 is highly expressed in cancer cells and enhances Wnt/β-catenin signaling.[23] TMEM9 directly binds to the subunit of v-ATPase and its accessory protein and accelerates the assembly of them, which provokes the vesicular acidification and the lysosomal APC degradation.[23] Moreover, genetic ablation of *Tmem9* suppresses intestinal tumorigenesis with down-regulation of Wnt/β-catenin signaling. β-catenin triggers transactivation of *TMEM9* and forms a positive-feedback loop, leading to the hyperactivation of Wnt/β-catenin signaling.[23] This interaction suggests that TMEM9 might amplify Wnt/β-catenin signaling in β-catenin/*CTNNB1*-mutated HCC and/or regenerative hepatocytes with increased Wnt/β-catenin signaling. Given the crucial role of Wnt/β-catenin signaling in tissue regeneration and tumorigenesis, potentially related to TMEM9, we herein sought to determine the biologic and pathologic roles of TMEM9 in liver regeneration and HCC.

Materials and Methods

CONSTRUCTS

All gene-expression plasmids were constructed from complementary DNA (cDNA) library or open reading frame sources using PCR and cloned into FLAG-pcDNA, FLAG-dTomato-pcDNA, FLAG-pLenti, or FLAG-Tomato-pLenti mammalian-expression

ARTICLE INFORMATION:

From the [1]Department of Experimental Radiation Oncology, Division of Radiation Oncology, The University of Texas MD Anderson Cancer Center, Houston, TX; [2]Department of Life Science, Chung-Ang University, Seoul, South Korea; [3]Department of Epigenetics and Molecular Carcinogenesis, The University of Texas MD Anderson Cancer Center, Houston, TX; [4]Department of Biomedical Sciences, College of Medicine, Inha University, Incheon, South Korea; [5]Graduate School of Biomedical Sciences, The University of Texas MD Anderson Cancer Center, Houston, TX; [6]Program in Genetics and Epigenetics, The University of Texas MD Anderson Cancer Center, Houston, TX.

ADDRESS CORRESPONDENCE AND REPRINT REQUESTS TO:

Jae-Il Park, Ph.D.
Department of Experimental Radiation Oncology, Division of Radiation Oncology, The University of Texas MD Anderson Cancer Center
Houston, TX 77030
E-mail: jaeil@mdanderson.org
Tel.: +1-713-792-3659

plasmids. Mutant constructs were generated by site-directed mutagenesis using PCR.

Tmem9 KNOCKOUT MOUSE ANIMAL MODEL

As in our previous study, the *Tmem9* KO mouse was established.[23] All animal procedures were performed based on the guidelines by the Association for the Assessment and Accreditation of Laboratory Animal Care and the Institutional (MD Anderson Cancer Center)–approved protocols (IACUC00001141; University of Texas MD Anderson Cancer Center Institutional Animal Care and Use Committee). The study is compliant with all relevant ethical regulations regarding animal research.

MAMMALIAN CELL CULTURE

Cell lines (Huh-7, HepG2, and HEK293T) were purchased from American Type Culture Collection and maintained in Dulbecco's modified Eagle medium (containing 10% fetal bovine serum and 1% penicillin-streptomycin). Mycoplasma screening was performed using the MycoAlert Mycoplasma Detection Kit (Lonza Group AG, Basel, Switzerland). Lentiviral plasmids encoding shRNAs were purchased from Open Biosystems (Huntsville, AL). To establish cell lines stably expressing shRNAs or genes, each cell line was transduced with lentiviruses and selected by puromycin (1-2 μg/mL) for 2 days. The following reagents were also used: CCl_4 (Sigma-Aldrich, St. Louis, MO), bafilomycin A1 (Wako Diagnostics), concanamycin A (Sigma-Aldrich), KM91104 (Millipore, Burlington, MA), CA074 (R&D Systems, Minneapolis, MN), and SID26681509 (R&D Systems).

REPORTER ASSAYS

The reporter plasmids, pMegaTOPFLASH and pMegaFOPFLASH, were transiently transfected with pSV40-Renilla plasmid (internal control) and analyzed using the Dual Luciferase assay system (Promega, Madison, WI).

APC SOMATIC CELL TARGETING

The APC KO cells were established using the clustered regularly interspaced short palindromic repeat (CRISPR) using a lentiviral CRISPR v2 vector (Addgene, Watertown, MA). The lentiviral plasmid contains two expression cassettes, hSpCas9 and the chimeric guide RNA (gRNA) where oligos were cloned, based on the protospacer adjacent motif on the target site. The lentiCRISPRv2 plasmids were transfected into HEK293T cells along with pCMV-ΔR8.2 dVPR and pCMV-VSVG plasmids for lentiviral packaging. HCC cell lines were then transduced with lentiviruses and selected in puromycin for 72 hours. After selection, three clonally selected cell lines were used for analysis. APC KO was confirmed by IB. The APC gRNA sequences were 5′- AGGATGGCTGCAGCTTCATA -3′ (#1) and 5′- GCAAGTTGAGGCACTGAAGA -3′ (#2).

IF STAINING AND IHC

Using percutaneous ethanol injection, cells were transiently transfected with plasmids. Cells grown on glass coverslips were washed and fixed in 4% paraformaldehyde for 10 minutes at 4°C. After blocking with 5% goat serum in phosphate-buffered saline (PBS) for 30 minutes, antibodies were treated for immunostaining cells. Liver samples were fixed in 10% neutral buffered formalin overnight and embedded in paraffin. Tissue samples were then sectioned (5 μm), and hematoxylin and eosin staining was performed following standard procedure. For IHC, slides were deparaffinized, rehydrated, processed for antigen retrieval, blocked, incubated with primary antibody, and fluorescence-conjugated secondary antibody. Next, slides were mounted with 4′,6-diamidino-2-phenylindole (DAPI; Invitrogen, Carlsbad, CA), sealed, and photographed using an inverted microscope (AxioVision; Zeiss, Oberkochen, Germany). For comparison among the experiment groups, images were captured with the same exposure time. The detailed information regarding antibodies can be found in Supporting Table S3.

GENE-EXPRESSION ANALYSIS

RNAs were extracted by TRIzol (Invitrogen) and converted to cDNAs using iScript cDNA synthesis kit (Bio-Rad Laboratories, Hercules, CA) with 1 μg of RNA. For gene-expression analysis, semi-quantitative RT-PCR or quantitative RT-PCR was performed. Quantitative RT-PCR results were quantified by comparative $2^{-\Delta\Delta Ct}$ methods (Applied Biosystems, Foster City, CA). For internal controls,

HPRT1 was used. The primer sequences can be found in Supporting Table S4.

IB AND IP

Whole-cell lysates of mammalian cells were prepared using NP-40 lysis buffer (0.5% NP-40, 1.5 mM MgCl2, 25 mM HEPES, 150 mM KCl, 10% glycerol, 1 mM phenylmethylsulfonyl fluoride, 12.7 mM benzamidine HCl, 0.2 mM aprotinin, 0.5 mM leupeptin, and 0.1 mM pepstatin A) for 20 minutes at 4˚C followed by centrifugation (14,000 rpm for 10 minutes). Supernatants were denatured in 5× sodium dodecyl sulfate (SDS) sample buffer (200 mM trishydroxymethylaminomethane [Tris]-HCl pH 6.8, 40% glycerol, 8% SDS, 200 mM dithiothreitol, and 0.08% bromophenol blue) at 95˚C for 5 minutes followed by SDS–polyacrylamide gel electrophoresis. For IB blocking and antibody incubation, 0.1% nonfat dry milk in Tris-buffered saline and Tween-20 (25 mM Tris-HCl pH 8.0, 125 mM NaCl, and 0.5% Tween-20) was used. SuperSignal West Pico (34087; ThermoFisher Scientific, Waltham, MA) and Femto (34095; ThermoFisher Scientific) reagents were used to detect horseradish peroxidase–conjugated secondary antibodies. For immunoprecipitation, cell lysates were incubated with 20 μL of magnetic beads (M8823; Sigma-Aldrich) for 2 hours. Immunoprecipitates were then washed with cell lysis buffer three times, eluted using an SDS sample buffer, and analyzed using IB. The detailed information regarding antibodies can be found in Supporting Table S3.

DUOLINK ASSAYS

For the visualization of protein interaction *in situ*, cells were seeded onto the cover glass. After fixation with 4% paraformaldehyde for 5 minutes, cells were permeabilized with 0.01% Triton-x100 for Duolink assays, according to the manufacturer's (DUO92101; Sigma-Aldrich) recommended protocol: blocking, primary antibody reaction, (+) and (−) probe reaction, ligation, polymerization, and amplification.

ACUTE CCl_4 INJURY MOUSE MODEL

Male mice (older than 8 weeks) were injected with CCl_4 (Sigma-Aldrich) for acute liver injury model. CCl_4 was dissolved in corn oil (Fisher Scientific) at a final concentration of 20% (v/v) for intraperitoneal administration (1 mL/kg). Mice were sacrificed at various time points, and liver tissues were collected for further analyses.

PHx IN MOUSE MODEL

PHx (70% removal of the total liver) or sham control surgery was performed with isoflurane anesthesia. Three to four WT C57BL/B6 and *Tmem9* KO (6 months of age) mice were used for PHx according to guidelines of the institutional Animal Care and Use Committee of the University of Texas, MD Anderson Cancer Center. Mice were sacrificed at 1 or 3 days after surgery, and remnant liver tissue was collected. Flash-frozen liver tissues were processed for RNA isolation, protein extraction, IHC, and mass.

XENOGRAFT ASSAYS

Mice (BALB/c nude) were subcutaneously injected with 5×10^6 cells of HepG2 cells (shCtrl vs. shTMEM9; shTMEM9-Vec vs. shTMEM-β-catenin; Ctrl vs. BAF [APC WT and KO]). After 3 weeks for adaptation, tumors were collected for assessment of tumor weight, RNA, IB, and IHC.

FRAP ASSAY

HepG2 cells were grown on chambered coverglass (Nunc) and were transfected with dTomato-β-catenin (WT and ΔN). After 24 hours transfection in 5% CO_2 at 37°C, images were acquired using a LSM880-Airyscan confocal (Zeiss). For photobleaching experiments, samples were photobleached with a solid-state laser using LSM880-Airyscan confocal. Nucleus was bleached for 1,000 seconds at 100% laser power. The samples were imaged every 5 seconds for 60 seconds with a separate 555 nm laser. The average fluorescence mean intensities of nucleus were measured using Zen software (Zeiss). The recovery curves shown are the averages of at least eight cells from at least three independent experiments.

IN SILICO ANALYSIS OF TMEM9 EXPRESSION AND GENETIC ALTERATION

TMEM9 expression in HCC cells was analyzed in the cBioPortal (www.cbioportal.org) and PICB database (www.Picb.ac.cn/PDXliver). The cBioPortal

analysis was performed with default options using the Cancer Genome Atlas (provisional and PanCancer) and Academic Medical Center data sets for gene alterations (mutations and copy number change).

CHROMATIN IMMUNOPRECIPITATION ASSAY

Cells were crosslinked with 1% formaldehyde for 15 minutes at room temperature, and quenched by glycine (0.125 M). After washing with cold PBS, tissues were incubated with lysis buffer (0.5% NP-40, 25 mM HEPES, 150 mM KCl, 1.5 mM $MgCl_2$, 10% glycerol, and KOH pH 7.5) containing protease inhibitor for 15 minutes on ice. Cell lysates were centrifuged (1,677*g* for 5 minutes), and supernatants were discarded. Cell pellets were subjected to sonication with nuclear lysis buffer (50 mM Tris pH 8.0, 10 mM ethylene diamine tetraacetic acid [EDTA], 1% SDS) using Bioruptor Plus sonication device (Diagenode). Supernatant was diluted 20 times in IP buffer (50 mM Tris pH 8.0, 150 mM NaCl, 0.5% NP-40, protease inhibitor mixtures) and subjected to IP with antibody against β-catenin or normal rabbit immunoglobulin G. Immunoprecipitates were also washed serially with chromatin immunoprecipitation (ChIP)–radio immunoprecipitation assay lysis buffer, high salt (50 mM Tris, pH 8.0; 500 mM NaCl; 0.1% SDS, 0.5% deoxycholate; 1% NP-40; and 1 mM EDTA), LiCl wash buffer (50 mM Tris, pH 8.0; 1 mM EDTA; 250 mM LiCl; 1% NP-40; and 0.5% deoxycholate) and Tris-EDTA buffer. Finally, immunoprecipitate crosslinking was reversed by incubation at 65°C overnight and treated with RNase A and proteinase K to extract the DNA. The ChIP PCR primer sequences of TMEM9 promoter amplicons was described in a previous paper. Glyceraldehyde 3-phosphate dehydrogenase promoter amplicons served as negative control.

CELL PROLIFERATION ASSAYS

Using plasmid stably expressing cells, the number of cells was counted using an hematocytometer to indicate growth days.

STATISTICS AND REPRODUCIBILITY

The Student *t* test was used to compare the two groups ($n \geq 3$). *P* values less than 0.05 were considered significant. Error bars indicate the SD, which indicates the SEM. All experiments were performed three or more times with similar results, independently, under identical or similar conditions.

ANTIBODY INFORMATION

See Supporting Table S3 for a complete list of antibodies.

PRIMER INFORMATION

See Supporting Table S4 for a complete list of primers.

Results

TMEM9 EXPRESSION DURING LIVER REGENERATION

The Wnt signaling is present in hepatocytes of the CV region, and not in the regenerating hepatocytes.[10-12] Given that TMEM9 positively regulates Wnt/β-catenin signaling, we first sought to locate TMEM9-expressing (TMEM9+) cells in the liver. Immunohistochemistry (IHC) showed that TMEM9+ cells were localized near the CV in normal mouse liver tissue but not *Tmem9* KO liver tissue (Fig. 1A).[23] TMEM9+ cells showed co-expression of glutamine synthetase (Gs), a marker for pericentral hepatocytes (Fig. 1B), but not cytokeratin 19 (Ck19), a marker for biliary epithelial cells (Fig. 1C). Next, we examined the expression of Tmem9 in the condition of liver regeneration by using a liver injury mouse model with CCl_4, a trigger for hepatocyte damage.[12,25] After CCl_4 administration, $Tmem9^{+/+}$ (wild-type [WT]) mice showed immediate loss of acutely pericentral hepatocytes, followed by gradual regeneration (Fig. 1D). Intriguingly, TMEM9+ cells immediately began repopulating after CCl_4 administration and culminated at 2 days following injury (days post-inoculation [dpi]; Fig. 1E), which was accompanied by an increase of Ki67+ cells (Fig. 1F). These results imply that TMEM9+ hepatocytes might be involved in hepatic regeneration.

IMPAIRED LIVER REGENERATION BY *Tmem9* KO

Having observed the expansion of TMEM9+ cells during hepatic regeneration, we asked whether

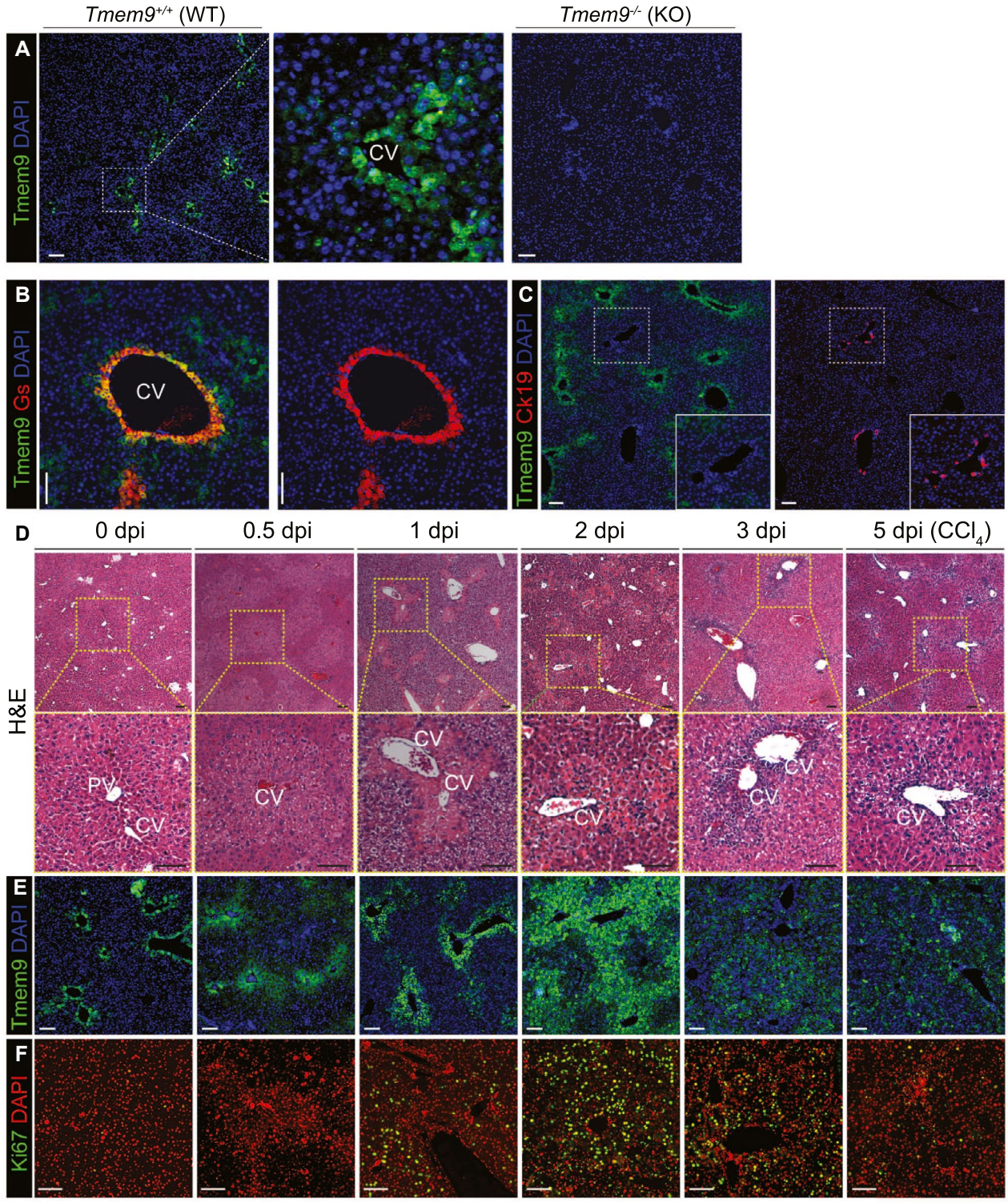

FIG. 1. Tmem9 expression during liver regeneration. (A-C) Tmem9+ cells are localized around the CV in the liver. IHC of mouse liver tissue for Tmem9 (A). *Tmem9* KO mouse liver tissue served as a negative control for Tmem9 IHC. Costaining for Tmem9 and glutamine synthetase, a marker for pericentral hepatocytes (B), or Ck19, a marker for biliary epithelial cells (C). (D,E) The number of Tmem9+ hepatocytes cells increases in regenerating liver tissue. After intraperitoneal injection of CCl_4, mouse liver tissue was analyzed by hematoxylin and eosin staining (D) and IHC for Tmem9 (E) and Ki67 (F). Representative images of three experiments with similar results. Scale bars = 100 μm. Abbreviation: PV, portal vein.

genetic ablation of *Tmem9* impairs hepatic regeneration. Because CCl_4-induced hepatic injury was mostly recovered at 3 dpi (see Fig. 1D-F), we investigated the effect of TMEM9 depletion on hepatic regeneration at 3 dpi in *Tmem9* KO mice, with *Tmem9* WT mice as controls. Of note, *Tmem9* KO mice exhibited no discernible phenotypes in the overall liver architecture and hepatocytes (Fig. 2A and Supporting Fig. S1A-F). Three days after CCl_4 administration, centrilobular necrosis was more severe in *Tmem9* KO mice than in *Tmem9* WT mice (Fig. 2B). Additionally, *Tmem9* KO liver tissue showed less cell proliferation near the CV (as indicated by Ki67-positive cells; Fig. 2C,D and Supporting Fig. S1G,H) without significant alteration of apoptosis (as indicated by cleaved caspase 3-positive cells; Supporting Fig. S1G,H). Given that regenerating cells near the CV differentiate into hepatocytes,[26,27] we examined the effect of TMEM9 depletion on hepatocyte expansion after liver injury using IHC for hepatocyte markers, hepatocyte nuclear factor 4α (Hnf4α), and albumin. Compared with *Tmem9* WT tissue, *Tmem9* KO mouse liver tissue showed the lower expression of Hnf4α and albumin at 3 dpi (Fig. 2E,F). Similarly, the expression of Wnt/β-catenin signaling-controlled markers, Gs, Tbx3 and Cyp2e1, was reduced and exhibited the delayed expression pattern in *Tmem9* KO mice compared to WT mice treated with CCl_4 (Fig. 2G,H and Supporting Fig. S1I). Also, *Tmem9* KO tissue showed a significantly smaller proportion of pericentral hepatocytes (as indicated by Gs-positive cells; Supporting Fig. S1G). These results suggest that TMEM9 is required for hepatic regeneration through repopulation of pericentral hepatocytes.

TMEM9-ACTIVATED WNT/β-CATENIN SIGNALING DURING LIVER REGENERATION

Next, we asked how TMEM9 contributes to hepatic regeneration. Given the active Wnt/β-catenin signaling in pericentral hepatocytes, which are TMEM9+ cells,[10,11] and the down-regulation of β-catenin target genes (Gs, Tbx3, and Cyp2e1) by *Tmem9* KO, we assessed the activity of Wnt/β-catenin signaling in the setting of liver injury by CCl_4 administration. Similar to TMEM9 up-regulation (Fig. 1E), β-catenin expression immediately increased and remained high until 2-3 dpi in normal mouse liver tissue, accompanied by increased cyclin D1 (Fig. 3A,B and Supporting Fig. S2A). Next, we analyzed the gene expression of several developmental pathways, including Wnt, Notch, Hedgehog, Hippo, and BMP. We found that *Tmem9* KO mouse liver tissue exhibited down-regulation of Wnt/β-catenin signaling target genes (*Axin2*, *Cd44*, and *Ccnd1*) after CCl_4 administration, whereas other target genes were not markedly affected (Fig. 3C). Similarly, *Tmem9* KO mouse liver tissue displayed lower expression levels of cyclin D1, Cd44, β-catenin, active β-catenin, and *Axin2*, compared with WT liver tissue (Fig. 3D-G and Supporting Fig. S2B), indicating that TMEM9 reinforces Wnt/β-catenin signaling in the setting of liver injury. TMEM9 hyperactivates Wnt/β-catenin signaling through APC degradation in colorectal cancer,[23] which next led us to ask whether TMEM9 negatively modulates APC even during liver regeneration. Indeed, we found higher levels of APC in *Tmem9* KO liver tissue, compared with WT liver tissue (Fig. 3H-L). Conversely, CCl_4-induced β-catenin up-regulation was reduced in *Tmem9* KO liver, compared with WT (Fig. 3L). These data indicate that TMEM9 promotes APC down-regulation during hepatic regeneration. In addition to CCl_4 injury model, we also used the partial hepatectomy (PHx) model to address the role of Tmem9 in liver regeneration. However, unlike CCl_4 injury, PHx did not up-regulate Tmem9 expression, and *Tmem9* KO did not impair PHx-induced liver regeneration (Supporting Fig. S3), indicating the essential role of Tmem9 in liver regeneration specifically in CV injury. Together, these results suggest that TMEM9 is required for the activation of Wnt/β-catenin signaling in regenerating liver tissue following CV injury.

EXPRESSION OF TMEM9 IN HCC

Wnt signaling is hyperactivated in HCC, with frequent mutations in the core components of Wnt signaling (β-catenin/*CTNNB1*, *AXIN*, and *APC*).[15,16] Having determined that TMEM9 is required for Wnt/β-catenin signaling activation during hepatic regeneration (see Fig. 3) with the implication of Wnt signaling hyperactivation, we explored the roles of TMEM9 in activating Wnt/β-catenin signaling in HCC. Interestingly, *in silico* analysis showed the

up-regulation of *TMEM9* transcripts in HCC compared with normal liver samples (Fig. 4A). Additionally, the *TMEM9* gene was frequently amplified in HCC (Fig. 4B), along with transcriptional up-regulation of *TMEM9* (Fig. 4C). HCC patient-derived xenograft samples also showed the amplification of *TMEM9*

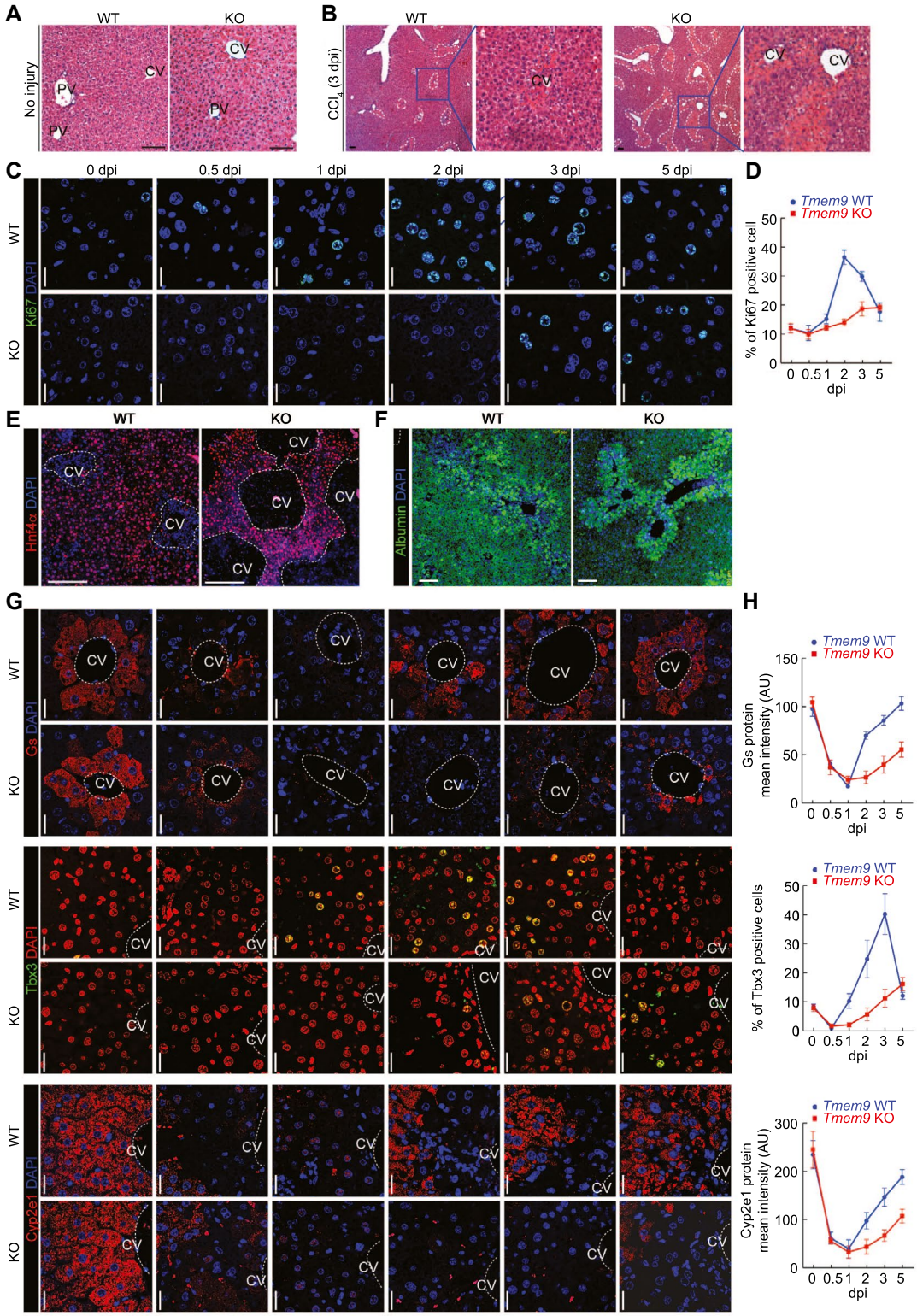

FIG. 2. Impaired liver regeneration by *Tmem9* knockout. (A) *Tmem9* KO impairs liver regeneration. In mice injected with control vehicle, no discernible phenotypes are seen in *Tmem9* KO hepatocytes. (B) After injection with CCl_4, centrilobular necrosis was more pronounced in *Tmem9* KO than in *Tmem9* WT mouse liver tissue. Dotted lines indicate the centrilobular necrosis region. (C) Cell proliferation was lower in *Tmem9* KO than in *Tmem9* WT mouse liver tissue following hepatic injury. (D) Staining of proliferating (Ki67) cells; quantification of Ki67+ cells. Hepatocyte expansion is down-regulated in *Tmem9* KO mice following hepatic injury. IHC for hepatocyte markers (Hnf4α [E] and albumin [F]) and pericentral hepatocytes. (G,H) Reduced and delayed expression of hepatocyte markers by *Tmem9* KO during liver regeneration. (G) IHC for Gs, Tbx3, and Cyp2e1. Quantification by ZEN software. Representative images of three experiments with similar results. Scale bars = 20 μm; error bars show mean ± SD from three or more independent experiments. Abbreviation: PV, portal vein.

gene (57%; 24 of 42) (Fig. 4D). cBioPortal (https://www.cbioportal.org) analysis showed that 32% of HCC samples displayed either gene amplification or transcriptional up-regulation of *TMEM9*, which was mutually exclusive to mutations of β-catenin/*CTNNB1* (28%) (Fig. 4E and Supporting Table S1). We also observed that β-catenin transactivates TMEM9 expression in HepG2 cells (Supporting Fig. S4A-C), consistent with colorectal cancer study. IHC of HCC and normal tissue microarrays confirmed the up-regulation of TMEM9 in HCC compared with normal liver tissues (Fig. 4F,G and Supporting Table S2). Furthermore, we examined the expression of TMEM9 in liver samples of patients with cirrhosis and found no significant association of TMEM9 expression with cirrhosis (Supporting Fig. S4C,D). These results suggest that TMEM9 expression is highly up-regulated in HCC, which implies the oncogenic roles of TMEM9 in hepatic tumorigenesis.

NUCLEAR TRANSLOCATION OF β-CATENIN BY TMEM9-DOWN-REGULATED APC

Given the overexpression of TMEM9 in HCC, we questioned the potential oncogenic roles of TMEM9 in HCC. To address this, we examined the effect of TMEM9 depletion on developmental pathways implicated in HCC. Quantitative reverse-transcription PCR (RT-PCR) analysis showed that TMEM9 depletion by short hairpin TMEM9 (shTMEM9) down-regulated Wnt/β-catenin target genes (*AXIN2* and *CD44*) in Huh-7 cells (Fig. 5A), indicating possible effects of TMEM9 on Wnt/β-catenin signaling in HCC. Because mutations of β-catenin/*CTNNB1* frequently occur in HCC,[15,16] we used β-catenin/*CTNNB1* WT Huh-7 cells and HepG2 cells carrying the exon 3-4 deleted β-catenin/*CTNNB1* allele to examine the effects of TMEM9 on Wnt/β-catenin signaling. In both β-catenin/*CTNNB1* WT and mutant cells, TMEM9 depletion (by shTMEM9) decreased β-catenin reporter activity (TOP/FOP FLASH luciferase) and *AXIN2* expression compared with control cells (Fig. 5B,C). In addition, TMEM9 depletion down-regulated the levels of total and active β-catenin protein (Fig. 5D) with cell growth inhibition (Supporting Fig. S5A), indicating that TMEM9 might be required for the maintenance of Wnt/β-catenin signaling activity regardless of β-catenin status (WT vs. mutant). Next, we directly tested the effect of TMEM9 on other mutant β-catenin cells (S33Y [non-phosphorylated active form] and ΔN [deletion of N-terminus 47 amino acids]), compared with WT cells. Surprisingly, TMEM9 depletion by short hairpin RNA (shRNA) decreased the levels of WT, S33Y, and ΔN β-catenin (Fig. 5E). Additionally, the rescue of WT and mutant β-catenin activated Wnt/β-catenin signaling and increased HCC cell proliferation, which was decreased by shTMEM9 (Fig. 5F and Supporting Fig. S5B-D). These results suggest that TMEM9 activates Wnt/β-catenin signaling independently of oncogenic mutations in β-catenin.

The protein destruction complex consisting of APC, CK1, AXIN, and GSK3 negatively regulates β-catenin by phosphorylation-mediated degradation of the β-catenin protein.[5] Serine/threonine residues of the N-terminus of β-catenin (Ser33, Ser37, Thr41, and Ser45) are sequentially phosphorylated by CK1 and GSK3, which is recognized by a β-TrCP E3 ligase. TMEM9 depletion decreased both WT and mutant β-catenin (S33Y and ΔN), implying that further negative regulator of β-catenin. Indeed, proteasome inhibitor (MG132) up-regulated WT and mutant β-catenin in *APC* KO-HepG2 cells. Moreover, we found ubiquitination of WT and mutant β-catenin in TMEM9-diminished cells (Supporting Fig. S5E-G), resulting in the possibility for APC destruction complex-independent proteasomal β-catenin degradation.

Moreover, the down-regulation of S33Y and ΔN-β-catenin by TMEM9 depletion might be explained by downstream events such as nuclear translocation of β-catenin or β-catenin's transcriptional activity. Thus, we asked whether TMEM9 affects the nuclear translocation of β-catenin. Immunofluorescence (IF)

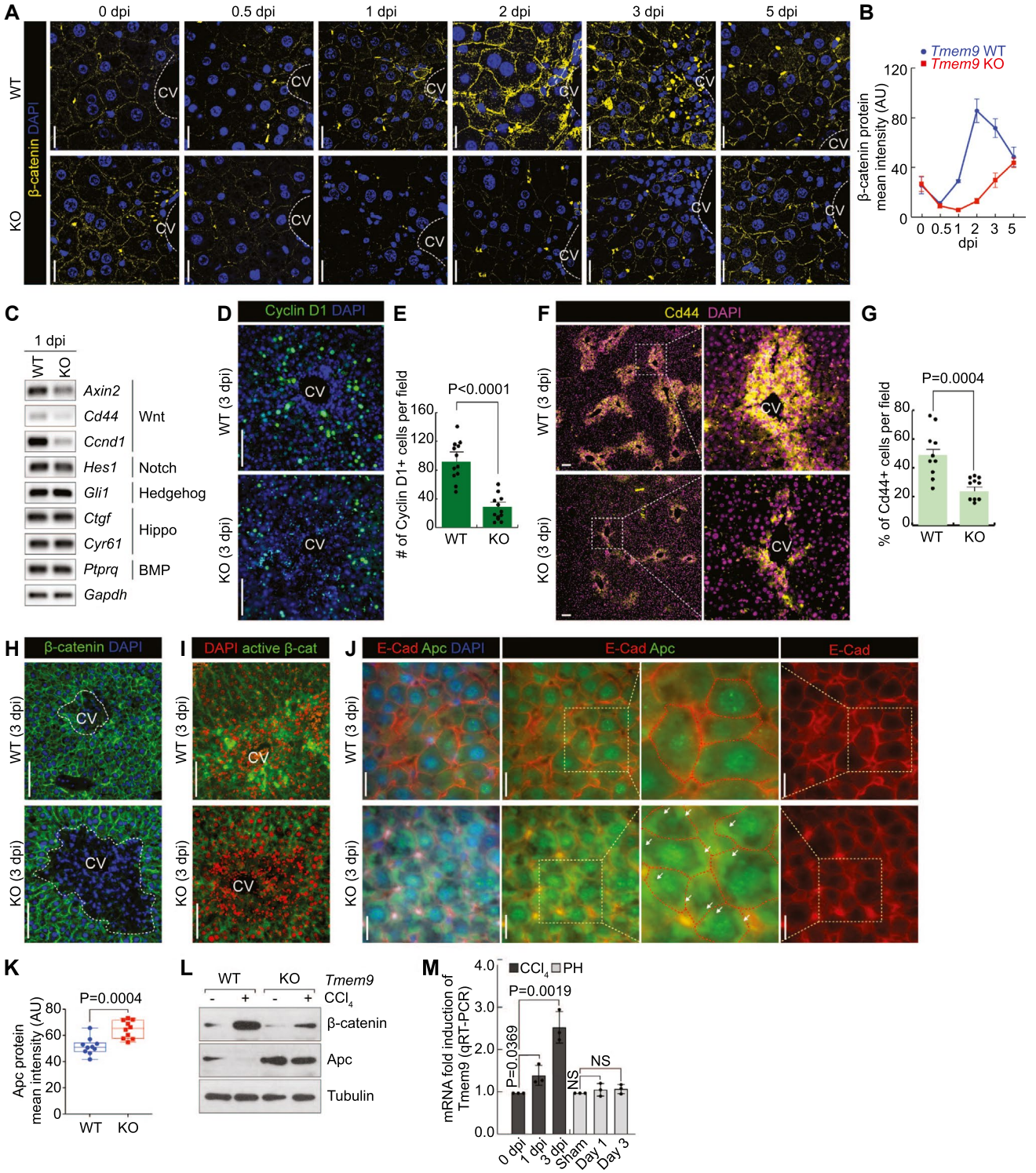

FIG. 3. TMEM9-activated Wnt/β-catenin signaling during liver regeneration. (A ,B) Wnt/β-catenin signaling is activated during liver regeneration. IHC for β-catenin in *Tmem9* WT and KO liver tissue after CCl_4 administration (A). To monitor β-catenin kinetics (B), liver tissues were collected at the indicated time. Scale bars = 20 μm. (C-G) *Tmem9* KO down-regulates Wnt/β-catenin signaling activity in regenerating liver tissue. Semiquantitative RT-PCR of *Tmem9* WT and KO mouse liver tissue at 1 dpi (C). The representative target genes of each signaling pathway were examined. IF staining for β-catenin target proteins cyclin D1 (D) and Cd44 (F). Quantification of cyclin D1+ (E) and Cd44+ (G) cells in *Tmem9* WT and KO liver at 3 dpi. Scale bars = 100 μm. (H,I) β-catenin levels are lower in *Tmem9* KO mouse liver tissue than in *Tmem9* WT tissue after hepatic injury. IHC for β-catenin (H) and active β-catenin (I). Scale bars = 100 μm. (J-L) *Tmem9* KO up-regulates Apc during liver regeneration following CCl_4-induced injury. IHC for E-cadherin and Apc (J). Arrows indicate the cytoplasmic accumulation of APC. Quantification of Apc by confocal microscopy (K). IB assays using *Tmem9* WT and*Tmem9* KO hepatocytes (L). Scale bars = 20 μm. (M) Increased *Tmem9* by CV region damage. After CCl_4 administration or PHx, tissues were collected at the indicated time point. quantitative RT-PCR for *Tmem9*. Representative images of three experiments with similar results; error bars indicate mean ± SD from at least three independent experiments. Abbreviations: *Ctgf*, connective tissue growth factor; GAPDH, glyceraldehyde 3-phosphate dehydrogenase; NS, not significant.

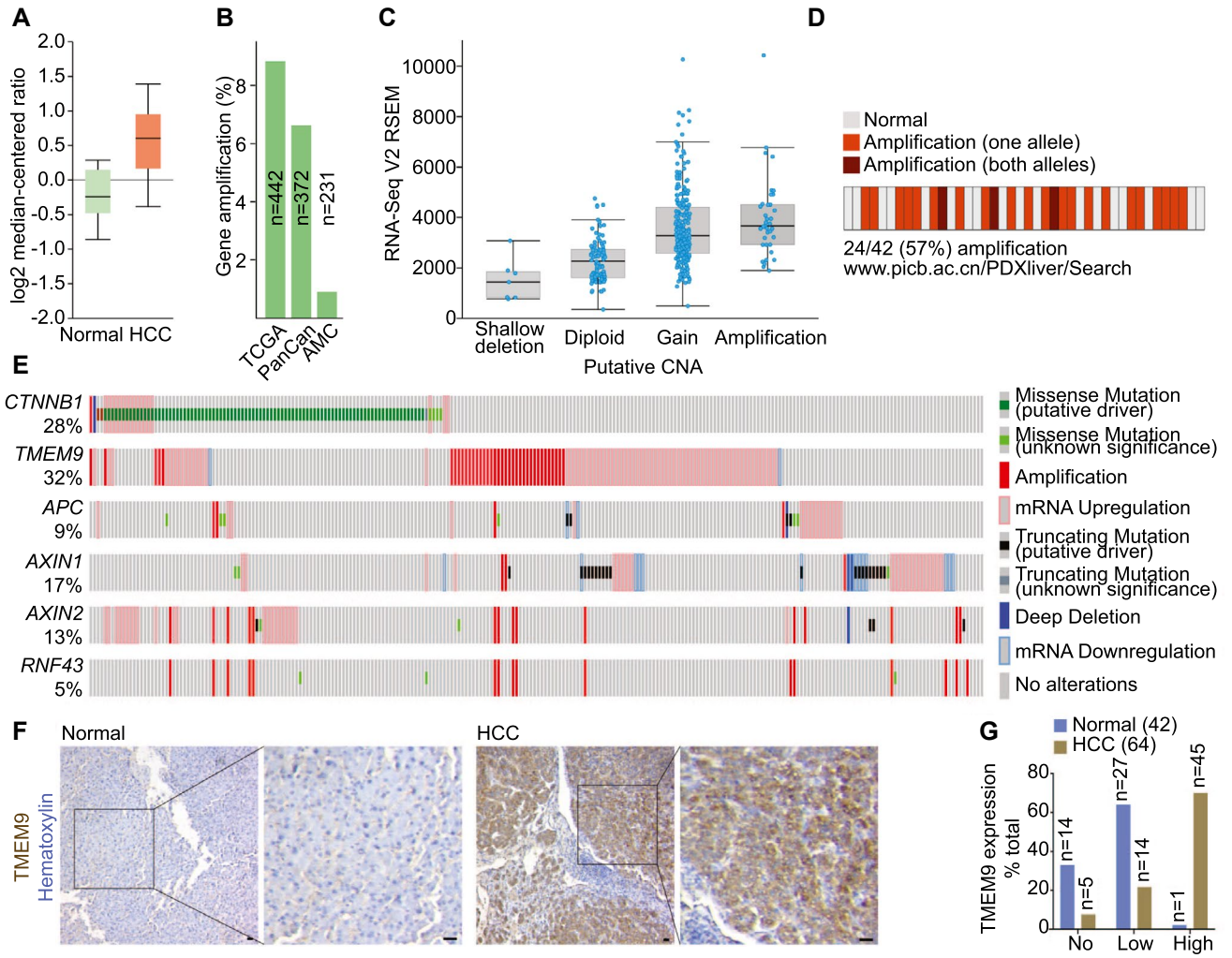

FIG. 4. Expression of TMEM9 in HCC. (A) *TMEM9* transcripts are up-regulated in HCC (cBioPortal analysis, www.cBioportal.org). (B) *TMEM9* gene amplification in HCC. cBioPortal analysis of the Cancer Genome Atlas, PanCan, and AMC data sets. (C) Relationship between gene amplification and transcriptional upregulation of *TMEM9* in HCC. (D) *TMEM9* amplification in HCC patient-derived xenograft (www.Picb.ac.cn/PDXliver). (E) Comparative visualization of HCC-related genetic and transcriptional alterations (cBioPortal analysis). (F) TMEM9 is up-regulated in HCC. IHC for TMEM9 in normal liver and HCC tissue microarrays. (G) Quantitative analysis of TMEM9 expression in normal liver and HCC samples. Representative images of three experiments with similar results. Scale bars = 100 μm. Abbreviations: RNA-Seq, RNA sequencing; TCGA, The Cancer Genome Atlas.

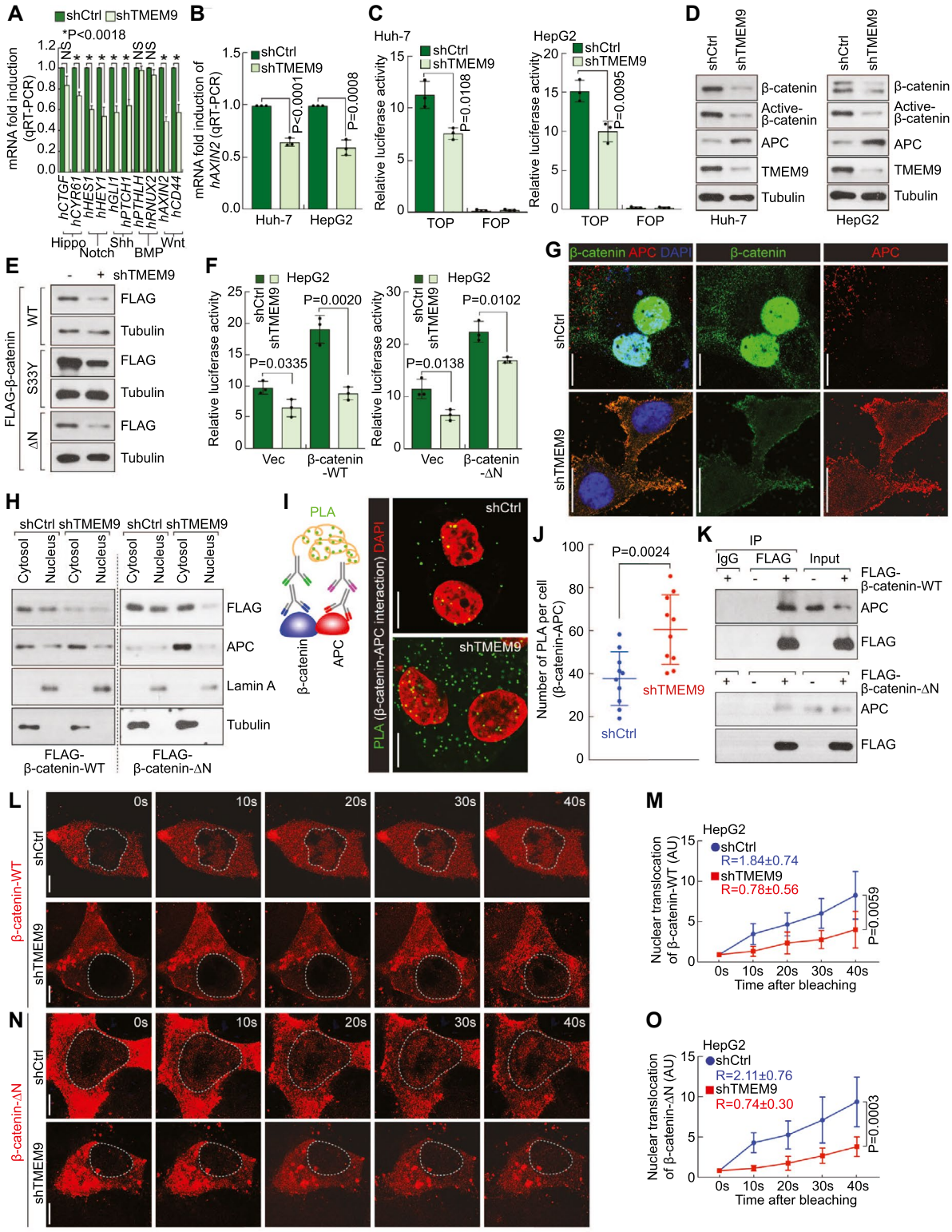
A
shCtrl shTMEM9
*P<0.0018
mRNA fold induction (qRT-PCR)
hCTGF hCYR61 hHES1 hHEY1 hGLI1 hPTCH1 hPTHLH hRNUX2 hAXIN2 hCD44
Hippo Notch Shh BMP Wnt
B
mRNA fold induction of hAXIN2 (qRT-PCR)
P<0.0001
P=0.0008
Huh-7 HepG2
C
Huh-7
HepG2
Relative luciferase activity
P=0.0108
P=0.0095
TOP FOP
D
shCtrl shTMEM9
β-catenin
Active-β-catenin
APC
TMEM9
Tubulin
Huh-7 HepG2
E
shTMEM9
FLAG-β-catenin
WT S33Y ΔN
FLAG
Tubulin
F
HepG2
Relative luciferase activity
P=0.0335
P=0.0020
P=0.0138
P=0.0102
Vec β-catenin-WT β-catenin-ΔN
G
β-catenin APC DAPI
β-catenin
APC
shCtrl
shTMEM9
H
shCtrl shTMEM9 shCtrl shTMEM9
Cytosol Nucleus Cytosol Nucleus Cytosol Nucleus Cytosol Nucleus
FLAG
APC
Lamin A
Tubulin
FLAG-β-catenin-WT
FLAG-β-catenin-ΔN
I
PLA
β-catenin
APC
PLA (β-catenin-APC interaction) DAPI
shCtrl
shTMEM9
J
P=0.0024
Number of PLA per cell (β-catenin-APC)
shTMEM9
shCtrl
K
IP
IgG FLAG Input
FLAG-β-catenin-WT
APC
FLAG
FLAG-β-catenin-ΔN
L
β-catenin-WT
shCtrl
shTMEM9
0s 10s 20s 30s 40s
M
HepG2
shCtrl
R=1.84±0.74
shTMEM9
R=0.78±0.56
P=0.0059
Nuclear translocation of β-catenin-WT (AU)
Time after bleaching
N
β-catenin-ΔN
O
HepG2
shCtrl
R=2.11±0.76
shTMEM9
R=0.74±0.30
P=0.0003
Nuclear translocation of β-catenin-ΔN (AU)
Time after bleaching

FIG. 5. Nuclear translocation of β-catenin by TMEM9-down-regulated APC. (A) TMEM9 depletion by shTMEM9 decreases expression of Wnt signaling target genes. Twenty-four hours after transfection, Huh-7 cells were analyzed by quantitative RT-PCR. (B,C) TMEM9 depletion decreases β-catenin transcriptional activity. Huh-7 and HepG2 cells were transfected with β-catenin reporter plasmids (pMega-TOP/FOP FLASH) for quantitative RT-PCR for *AXIN2* (B) and luciferase assays (C). (D,E) TMEM9 depletion down-regulates β-catenin protein in HCC cells. After 24-hour transfection, endogenous β-catenin (D) and ectopically expressed β-catenin (WT) and mutants (S33Y and ΔN) (E) were assessed by IB assays. (F) shTMEM9 reduces WT and mutant β-catenin transcriptional activity. Huh-7 and HepG2 cells were transfected with WT or mutant (ΔN) β-catenin plasmid. Luciferase (TOP/FOP FLASH) was measured to determine β-catenin transcriptional activity. (G) TMEM9 depletion inhibits nuclear translocation of β-catenin. IF staining for β-catenin and APC. (H) After 24-hour transfection with WT or ΔN β-catenin plasmid, HepG2 cells were fractionated into cytosolic and nuclear fractions, followed by IB. Scale bars = 20 μm. (I) shTMEM9 increases interaction between APC and β-catenin. Illustration of APC-β-catenin binding assay using Duolink PLA (left); green PLA fluorescence indicates APC-β-catenin interaction (right). (J) Quantification of PLA. Scale bars = 10 μm. (K) Binding between APC and WT or mutant β-catenin. Co-immunoprecipitation analysis. (L-O) Depletion of TMEM9 restrains nuclear translocation of β-catenin. HepG2 cells were transfected with a tdTomato-3xFLAG-β-catenin plasmid (WT or ΔN) for 24 hours. Nuclear fluorescence of β-catenin was bleached for 1,000 seconds, followed by visualization (L,N) and quantification for mean intensity (M,O) by confocal microscopy every 10 seconds. Quantification was normalized by the nuclear mean intensity of 0 seconds. *R* values indicate the velocity of β-catenin nuclear translocation. Scale bars = 5 μm. Representative images of three experiments with similar results; error bars show the mean ± SD from at least three independent experiments; two-sided unpaired *t* test. Abbreviations: IgG, immunoglobulin G; NS, not significant; qRT-PCR, quantitative RT-PCR; Vec, empty vector plasmid-transfected control.

staining and cytosol/nuclear fractionation assays showed that endogenous β-catenin was localized primarily in the nuclei of HepG2 cells, and this nuclear localization of β-catenin was decreased by TMEM9 depletion (Fig. 5G,H and Supporting Fig. S5H). These results indicate that TMEM9 is required for nuclear translocation of β-catenin independently of mutations in β-catenin.

In addition to its role in β-catenin degradation, APC has been shown to control the level of nuclear β-catenin.[28,29] TMEM9 also down-regulates APC through v-ATPase-mediated lysosomal degradation.[23] Therefore, we next asked whether TMEM9 depletion increases APC-β-catenin interaction regardless of the mutation status of β-catenin. As expected, the Duolink proximity ligation assay (PLA)[30] revealed that shTMEM9 increased the association between APC and β-catenin in HepG2 cells (Fig. 5I,J). Co-immunoprecipitation assays also showed the interaction between APC and β-catenin (WT, S33Y, and ΔN; Fig. 5K and Supporting Fig. S1F). Because it has been reported that APC induces cytoplasmic retention of β-catenin,[31] we examined the effect of shTMEM9 on nuclear localization of WT and mutant β-catenin using fluorescence recovery after photobleaching (FRAP) assay. Intriguingly, shTMEM9 decreased the nuclear import of WT and mutant β-catenin (Fig. 5L-O). These results suggest that TMEM9 increases the nuclear localization of β-catenin by inhibiting APC-induced β-catenin cytoplasmic retention.

TMEM9-INDUCED ACTIVATION AND NUCLEAR TRANSLOCATION OF β-CATENIN BY LYSOSOMAL DEGRADATION OF APC

Previously, we found that TMEM9 activates v-ATPase, which subsequently induces vesicular acidification for the lysosomal protein degradation of APC.[23] Given the increased APC and the retention of β-catenin by TMEM9 depletion in HCC cells (Fig. 5), we tested whether lysosomal protein degradation of APC mediates TMEM9-activated β-catenin using lysosomal inhibitors. Indeed, the lysosomal protease inhibitors CA074 (an inhibitor of cathepsin B [CTB])[32] and SID26681509 (an inhibitor of cathepsin L)[33] decreased levels of both WT and mutant β-catenin protein, *AXIN2* expression, luciferase activity, and HCC cell proliferation, but increased the level of APC protein, in Huh-7 and HepG2 cells (Fig. 6A,B and Supporting Fig. S6). Likewise, lysosomal protease inhibitors also down-regulated the level of ectopically expressed WT and mutant β-catenin (Fig. 6C). Because of the cytosolic retention of β-catenin by APC (see Fig. 5L-O), we also assessed the effects of lysosomal protease inhibitors on the nuclear translocation of β-catenin. Cytosolic and nuclear fractionation followed by immunoblot (IB) and IF assays showed that lysosomal protease inhibitors prevented nuclear translocation of WT and mutant β-catenin (Fig. 6D,F). We also found that lysosomal protease

inhibitors augmented APC-β-catenin interaction in HepG2 cells (PLA; Fig. 6G,H). Furthermore, we tested whether the APC protein is localized in the lysosome. Indeed, PLA assay showed co-localization of APC with LAMP1, a lysosomal marker, and this co-localization was increased by TMEM9

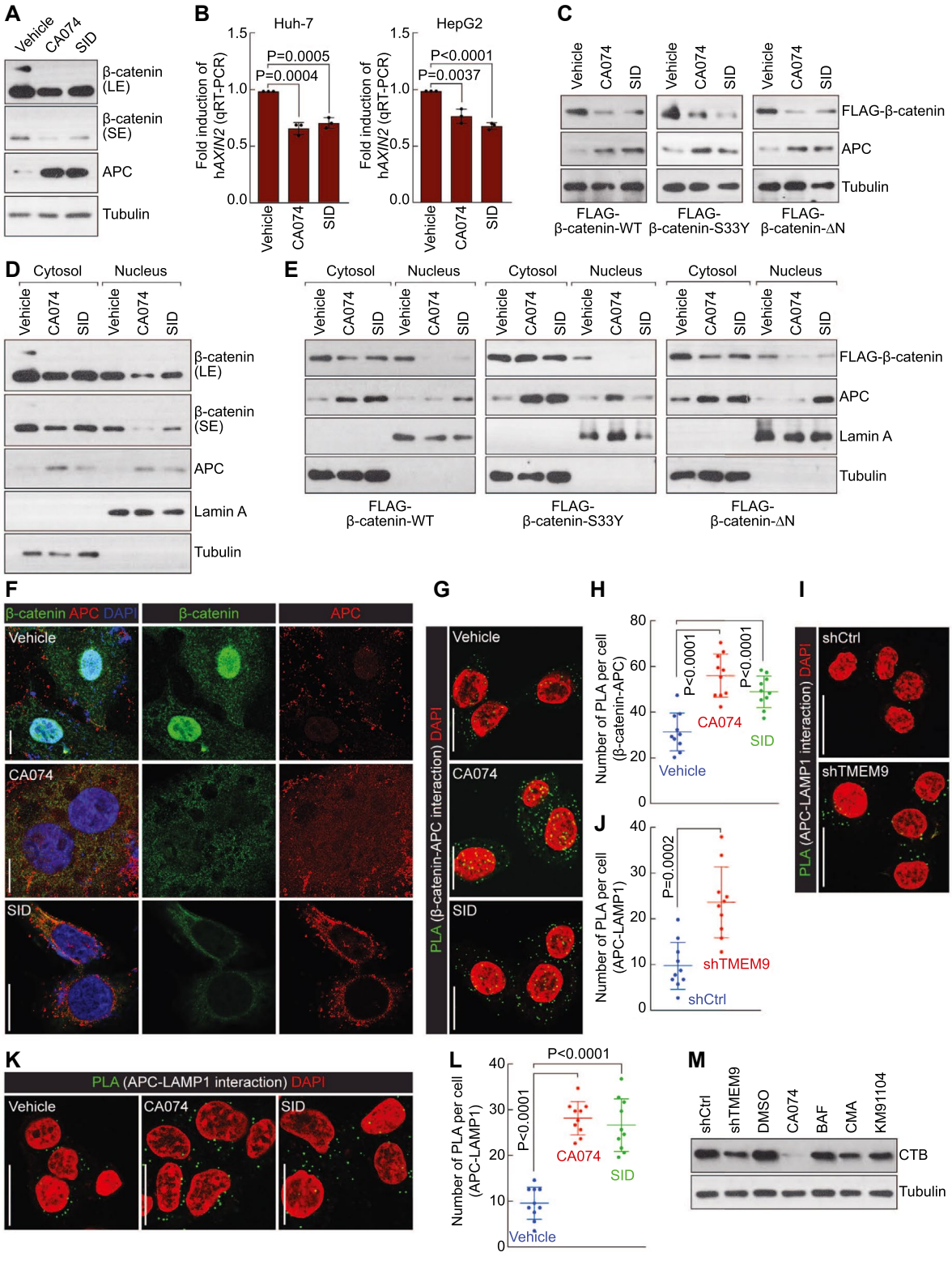

FIG. 6. TMEM9-induced activation and nuclear translocation of β-catenin by lysosomal degradation of APC. (A) Lysosomal protease inhibitors down-regulate β-catenin protein. HepG2 cells were treated with CA074 (5 μM) or SID (SID26681509; 50 nM) for 12 hours. IB assays. (B) Lysosomal protease inhibitors decrease β-catenin transcriptional activity. Quantitative RT-PCR for *AXIN2*. (C) Lysosomal protease inhibitors deplete ectopically expressed WT and mutant β-catenin. After transfection with WT, S33Y, or ΔN β-catenin plasmid, HepG2 cells were treated with CA074 or SID. (D-F) Lysosomal protease inhibitors restrict nuclear translocation of β-catenin. Cytosol/nuclear fractionation (D,E). (F) IF staining for β-catenin and APC. (G,H) Lysosomal protease inhibitors increase interaction between APC and β-catenin: Duolink assays (G) and quantification of PLA (H). (I,J) TMEM9 depletion upregulates lysosomal APC. Duolink assay using APC and LAMP1 antibodies (I). LAMP1 served as a lysosomal marker. Quantification of APC-LAMP1 co-localization (J). (K,L) Lysosomal protease inhibitors increase lysosomal APC. Duolink assay (K) and quantification of interaction between APC and LAMP1 (L). (M) TMEM9 depletion down-regulates cathepsin maturation. HepG2 cells were transfected with shTMEM9 or treated with indicated v-ATPase and lysosomal protease inhibitors BAF (bafilomycin A1, 3 nM), CMA (concanamycin A, 0.3 nM), or KM91104 (10 μM). Representative images of three experiments with similar results. Scale bars = 20 μm; error bars show the mean ± SD from at least three independent experiments; two-sided unpaired *t* test. Abbreviations: LE, long exposure; SE, short exposure.

depletion (Fig. 6I,J) and lysosomal protease inhibitors (Fig. 6K,L). These results suggest that TMEM9 down-regulates APC through lysosomal degradation of APC protein.

TMEM9 facilitates the assembly of v-ATPase and increases the vesicular acidification, which is essential for lysosome-mediated protein degradation.[34,35] CTB is a widely presented lysosomal cysteine protease, and loss of CTB leads to lysosomal dysfunction.[36,37] CTB is produced from a large precursor form (pro-CTB) to form a mature cathepsin containing a heavy and a light chain. Thus, we examined the effects of TMEM9 on lysosomal integrity by measuring the amount of mature CTB. In HepG2 cells, TMEM9 depletion and inhibitors of v-ATPase and lysosomal protease decreased the level of mature CTB (Fig. 6M), indicating that TMEM9 is required for lysosomal function. These results suggest that TMEM9 activates β-catenin through lysosomal degradation of APC in HCC.

SUPPRESSION OF HEPATIC TUMORIGENESIS BY BLOCKADE OF TMEM9-v-ATPase-APC SIGNALING AXIS

Having determined the oncogenic roles of TMEM9-v-ATPase signaling axis in liver cancer cell proliferation, next we tested the effects of blockade of TMEM9-v-ATPase axis on *in vivo* tumorigenesis. We subcutaneously injected HepG2 cells (shCtrl, shTMEM9, shTMEM9 + β-catenin, and *APC* WT vs. KO) into the immunocompromised mice and monitor tumor growth. We found that TMEM9-depleted HepG2 (shTMEM9) cells showed the inhibition of tumor development, compared with the control (shCtrl) HepG2 cells (Fig. 7A). Similarly, *AXIN2*, a β-catenin target gene, expression was reduced by TMEM9 depletion, while APC was up-regulated (Fig. 7A). Next, we asked whether TMEM9 depletion–induced HCC growth inhibition is due to the decreased Wnt/β-catenin signaling activity by the rescue experiments. Indeed, β-catenin ectopically expressing cells restored *in vivo* tumor development suppressed by TMEM9 depletion, along with the up-regulation of *AXIN2* (Fig. 7B). However, APC level was not affected by β-catenin ectopic expression (Fig. 7B). Additionally, we tested the effects of v-ATPase inhibitor, bafilomycin (BAF), on *in vivo* tumorigenesis. Similar to TMEM9 knockdown using shRNA, BAF treatment inhibited *in vivo* tumorigenesis, *AXIN2* expression, but increased APC (Fig. 7C). Next, to test whether the tumor inhibitory effects of BAF are due to APC up-regulation, we established *APC* KO-HepG2 cells (Supporting Fig. S7A,B) and tested whether BAF also inhibits tumorigenesis of *APC* KO cells. Consistent with the *in vitro* results (Supporting Fig. S7C,D), BAF did not suppress *in vivo* tumorigenesis of *APC* KO and did not affect *AXIN2* expression (Fig. 7D). These results strongly suggest the tumorigenic roles of TMEM9-v-ATPase axis in HCC through Wnt/β-catenin signaling hyperactivation.

Discussion

Herein, we found that TMEM9 contributes to hepatic regeneration and tumorigenesis by activating the Wnt/β-catenin pathway.

The APC destruction complex down-regulates β-catenin through phosphorylation (Ser 34, Ser 37,

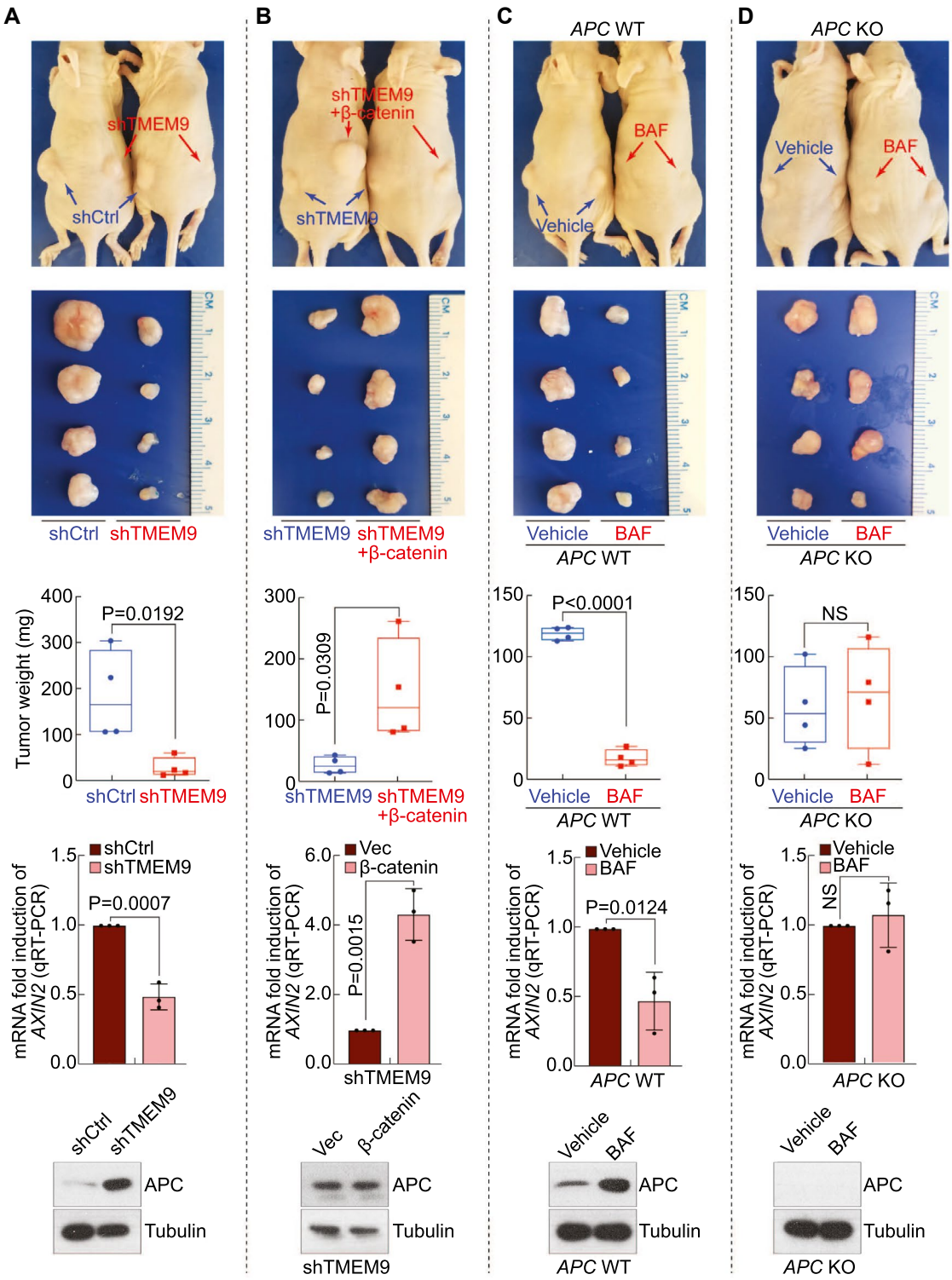

FIG. 7. Inhibition of *in vivo* hepatic tumorigenesis by blockade of TMEM9-v-ATPase axis. (A-D) Inhibition of *in vivo* tumor development by TMEM9 depletion (shTMEM9) or BAF. (A) HepG2 (shCtrl vs. shTMEM9). (B) Vector control versus β-catenin (shTMEM9-HepG2). (C) Vehicle versus BAF, *APC* WT. (D) *APC* KO. Cells were subcutaneously injected into the left and right flank of immunocompromised mice (BALB/c nude). Three weeks after injection, tumorigenesis was analyzed by assessing tumor weight, Wnt/β-catenin signaling activity (quantitative RT-PCR for *AXIN2*), and APC protein expression (IB). BAF (0.5 mg/kg): every 3 days for 21 days. Abbreviation: NS, not significant.

Thr 41, and Ser 45 of β-catenin)–based proteasomal degradation.[5] APC also modulates the nuclear import and export of β-catenin, leading to cytoplasmic retention of β-catenin to inhibit Wnt target gene transactivation.[28,29,31] In cancer cells, nonsense mutations in *APC* or missense mutations in β-catenin/*CTNNB1* hyperactivate Wnt/β-catenin target gene transactivation, contributing to tumorigenesis. The conventional view on APC loss–activated β-catenin in cancer cells is that inactivation of APC stabilizes the β-catenin protein and subsequent nuclear translocation of β-catenin. However, recent studies suggested that β-catenin can still be inhibited in cells carrying mutations in *APC* or β-catenin/*CTNNB1*.[22] In agreement with these studies, we recently reported that mutant APC protein binds to and interferes with β-catenin-mediated gene transactivation.[23] Consistent with this, we found that APC protein induces the cytosolic retention of both WT and mutant β-catenin in HCC cells (Fig. 6L-O), which indicates that APC down-regulates Wnt/β-catenin signaling activity through dual regulatory mechanisms: proteasomal degradation and cytosolic retention of β-catenin.

Wnt signaling is activated in pericentral hepatocyte during liver homeostasis and regeneration.[10-12] In a CCl_4-induced liver injury model using *Tmem9* WT and *Tmem9* KO mice, we found that TMEM9+ cells were located primarily among the pericentral hepatocytes, and the number of TMEM9+ cells increased following liver injury. Although *Tmem9* KO mice are viable without defects in liver development,[23] *Tmem9* KO showed defects in hepatocyte regeneration with the defects on Wnt signaling activation following liver injury. Consistent with HCC results, *Tmem9* KO liver tissue showed higher expression of APC than did *Tmem9* WT liver tissue. Additionally, the CCl_4-induced liver injury model showed increased β-catenin levels through APC down-regulation. It should also be noted that Tmem9 is not up-regulated by PHx injury, and *Tmem9* KO does not affect PHx-induced regeneration. These results suggest that TMEM9 down-regulates APC to activate Wnt/β-catenin signaling for hepatic regeneration somehow specific to CV injury.

The metabolic zonation, a spatial and functional organization of liver, is controlled by several processes including APC protein.[38-42] However, it remains unclear how the level of APC is modulated for metabolic zonation. TMEM9-induced lysosomal degradation of APC might explain the differential gradient of APC protein for zonation. However, despite the up-regulation of Apc by *Tmem9* genetic ablation (Fig. 3L and Supporting Fig. S1A), *Tmem9* KO mice display no aberrant liver defects in development and homeostasis, which might be due to the intrinsic compensatory mechanisms of Wnt/β-catenin signaling.[43-45] However, following CCl_4 injury when immediate cell mitogenic and reprogramming occur, *Tmem9* KO mice displayed the overall down-regulation and delayed expression of Wnt/β-catenin signaling and hepatocyte markers, along with the impaired zonation (Figs. 2G and 3A, and Supporting Fig. S1I). Thus, the process in which TMEM9 transactivated by β-catenin amplifies Wnt/β-catenin signaling is specifically required for metabolic zonation only in regeneration condition but not during liver development and homeostasis.

v-ATPase inhibitors such as bafilomycin A1, concanamycin A, and KM91104 exhibit tumor-suppressive effects in various human cancers.[23,46-50] Interestingly, these cancers exhibit amplified TMEM9 expression. For example, HCC cells frequently harbor *TMEM9* gene amplification (Fig. 4). Thus, it is plausible that v-ATPase inhibition may be an effective therapeutic option for TMEM9-catenin and Wnt/β-catenin signaling-dependent cancers.

In the MVBs, v-ATPase controls vesicle acidification. Among of the serine, aspartic, and lysosomal cysteine proteases, lysosomal cysteine cathepsins such as cathepsin B and L require an acidic environment to be active,[34,35] which suggests that v-ATPase likely plays a crucial role in activating cathepsin in the lysosomes. Indeed, shTMEM9-reduced v-ATPase activity and v-ATPase inhibitors restrained cathepsin maturation (Fig. 6M). Because cathepsin B and L are highly expressed in human cancer and associated with cell invasion through matrix metalloproteinase activation,[51,52] the potential roles of TMEM9 in cancer invasion and metastasis need to be addressed in the future. Moreover, given that v-ATPase positively controls MVB acidification and lysosomal degradation, other signaling pathways may also be affected by TMEM9. Despite our main focus on Wnt/β-catenin signaling, other signaling possibly controlled by TMEM9-v-ATPase-lysosome should also be studied.

Together, our results revealed that TMEM9 induces lysosomal degradation of APC by promoting

lysosomal protease maturation, which is indispensable for liver regeneration and tumorigenesis. Moreover, we discovered that APC inhibits Wnt signaling by cytosolic retention of β-catenin independently of β-catenin's oncogenic mutations.

Acknowledgment: The authors thank Pierre D. McCrea for the constructive comments on the manuscript.

Author Contributions: Y.-S.J., S.A.S., S.H.L., and J.-I.P. were responsible for the study design. Y.-S.J., S.A.S., S.H.L., M.J.K., S.J., J.Z., C.L.C., J.-H.C., and J.-I.P. were responsible for performing the experiments. Y.-S.J., S.A.S., S.H.L., M.J.K., M.C.B., and J.-I.P. were responsible for the data analysis. Y.-S.J., S.H.L., and J.-I.P. were responsible for the manuscript writing.

REFERENCES

1) Schlessinger K, Hall A, Tolwinski N. Wnt signaling pathways meet Rho GTPases. Genes Dev 2009;23:265-277.
2) Ouyang H, Zhuo Y, Zhang K. WNT signaling in stem cell differentiation and tumor formation. J Clin Invest 2013;123: 1422-1424.
3) Russell JO, Monga SP. Wnt/beta-catenin signaling in liver development, homeostasis, and pathobiology. Annu Rev Pathol 2018;13:351-378.
4) Clevers H, Nusse R. Wnt/beta-catenin signaling and disease. Cell 2012;149:1192-1205.
5) Stamos JL, Weis WI. The beta-catenin destruction complex. Cold Spring Harb Perspect Biol 2013;5:a007898.
6) Monga SP, Pediaditakis P, Mule K, Stolz DB, Michalopoulos GK. Changes in WNT/beta-catenin pathway during regulated growth in rat liver regeneration. Hepatology 2001;33:1098-1109.
7) Sekine S, Gutierrez PJ, Lan BY, Feng S, Hebrok M. Liver-specific loss of beta-catenin results in delayed hepatocyte proliferation after partial hepatectomy. Hepatology 2007;45:361-368.
8) Sodhi D, Micsenyi A, Bowen WC, Monga DK, Talavera JC, Monga SP. Morpholino oligonucleotide-triggered beta-catenin knockdown compromises normal liver regeneration. J Hepatol 2005;43:132-141.
9) Tan X, Behari J, Cieply B, Michalopoulos GK, Monga SP. Conditional deletion of beta-catenin reveals its role in liver growth and regeneration. Gastroenterology 2006;131:1561-1572.
10) Wang B, Zhao L, Fish M, Logan CY, Nusse R. Self-renewing diploid Axin2(+) cells fuel homeostatic renewal of the liver. Nature 2015;524:180-185.
11) Itoh T, Kamiya Y, Okabe M, Tanaka M, Miyajima A. Inducible expression of Wnt genes during adult hepatic stem/progenitor cell response. FEBS Lett 2009;583:777-781.
12) Zhao L, Jin Y, Donahue K, Tsui M, Fish M, Logan CY, et al. Tissue repair in the mouse liver following acute carbon tetrachloride depends on injury-induced Wnt/beta-catenin signaling. Hepatology 2019;69:2623-2635.
13) Nejak-Bowen KN, Monga SP. Beta-catenin signaling, liver regeneration and hepatocellular cancer: sorting the good from the bad. Semin Cancer Biol 2011;21:44-58.
14) Fukutomi T, Zhou Y, Kawai S, Eguchi H, Wands JR, Li J. Hepatitis C virus core protein stimulates hepatocyte growth: correlation with upregulation of wnt-1 expression. Hepatology 2005;41:1096-1105.
15) **de La Coste A**, **Romagnolo B**, Billuart P, Renard CA, Buendia MA, Soubrane O, et al. Somatic mutations of the beta-catenin gene are frequent in mouse and human hepatocellular carcinomas. Proc Natl Acad Sci U S A 1998;95:8847-8851.
16) **Satoh S**, **Daigo Y**, Furukawa Y, Kato T, Miwa N, Nishiwaki T, et al. AXIN1 mutations in hepatocellular carcinomas, and growth suppression in cancer cells by virus-mediated transfer of AXIN1. Nat Genet 2000;24:245-250.
17) Monga SP. Beta-catenin signaling and roles in liver homeostasis, injury, and tumorigenesis. Gastroenterology 2015;148:1294-1310.
18) **Vermeulen L**, **De Sousa EMF**, van der Heijden M, Cameron K, de Jong JH, Borovski T, et al. Wnt activity defines colon cancer stem cells and is regulated by the microenvironment. Nat Cell Biol 2010;12:468-476.
19) Goentoro L, Kirschner MW. Evidence that fold-change, and not absolute level, of beta-catenin dictates Wnt signaling. Mol Cell 2009;36:872-884.
20) Koo BK, Spit M, Jordens I, Low TY, Stange DE, van de Wetering M, et al. Tumour suppressor RNF43 is a stem-cell E3 ligase that induces endocytosis of Wnt receptors. Nature 2012;488:665-669.
21) Jung YS, Jun S, Lee SH, Sharma A, Park JI. Wnt2 complements Wnt/beta-catenin signaling in colorectal cancer. Oncotarget 2015;6:37257-37268.
22) **Voloshanenko O**, **Erdmann G**, Dubash TD, Augustin I, Metzig M, Moffa G, et al. Wnt secretion is required to maintain high levels of Wnt activity in colon cancer cells. Nat Commun 2013;4:2610.
23) Jung YS, Jun S, Kim MJ, Lee SH, Suh HN, Lien EM, et al. TMEM9 promotes intestinal tumorigenesis through vacuolar-ATPase-activated Wnt/beta-catenin signalling. Nat Cell Biol 2018;20:1421-1433.
24) Kveine M, Tenstad E, Døsen G, Funderud S, Rian E. Characterization of the novel human transmembrane protein 9 (TMEM9) that localizes to lysosomes and late endosomes. Biochem Biophys Res Commun 2002;297:912-917.
25) Boll M, Weber LW, Becker E, Stampfl A. Mechanism of carbon tetrachloride-induced hepatotoxicity. Hepatocellular damage by reactive carbon tetrachloride metabolites. Z Naturforsch C 2001;56:649-659.
26) Fausto N, Campbell JS. The role of hepatocytes and oval cells in liver regeneration and repopulation. Mech Dev 2003;120:117-130.
27) Oh SH, Witek RP, Bae SH, Zheng D, Jung Y, Piscaglia AC, et al. Bone marrow-derived hepatic oval cells differentiate into hepatocytes in 2-acetylaminofluorene/partial hepatectomy-induced liver regeneration. Gastroenterology 2007;132:1077-1087.
28) Henderson BR, Fagotto F. The ins and outs of APC and beta-catenin nuclear transport. EMBO Rep 2002;3:834-839.
29) Henderson BR. Nuclear-cytoplasmic shuttling of APC regulates beta-catenin subcellular localization and turnover. Nat Cell Biol 2000;2:653-660.
30) Weibrecht I, Leuchowius KJ, Clausson CM, Conze T, Jarvius M, Howell WM, et al. Proximity ligation assays: a recent addition to the proteomics toolbox. Expert Rev Proteomics 2010;7:401-409.
31) Wang L, Liu X, Gusev E, Wang C, Fagotto F. Regulation of the phosphorylation and nuclear import and export of beta-catenin by APC and its cancer-related truncated form. J Cell Sci 2014;127:1647-1659.
32) Montaser M, Lalmanach G, Mach L. CA-074, but not its methyl ester CA-074Me, is a selective inhibitor of cathepsin B within living cells. Biol Chem 2002;383:1305-1308.
33) **Shah PP**, **Wang T**, Kaletsky RL, Myers MC, Purvis JE, Jing H, et al. A small-molecule oxocarbazate inhibitor of human cathepsin L blocks severe acute respiratory syndrome and ebola pseudotype virus infection into human embryonic kidney 293T cells. Mol Pharmacol 2010;78:319-324.

34) Turk V, Stoka V, Vasiljeva O, Renko M, Sun T, Turk B, et al. Cysteine cathepsins: from structure, function and regulation to new frontiers. Biochim Biophys Acta 2012;1824:68-88.
35) Turk B, Turk D, Turk V. Lysosomal cysteine proteases: more than scavengers. Biochim Biophys Acta 2000;1477:98-111.
36) **Qi X**, **Man SM**, Malireddi RK, Karki R, Lupfer C, Gurung P, et al. Cathepsin B modulates lysosomal biogenesis and host defense against Francisella novicida infection. J Exp Med 2016;213:2081-2097.
37) Cermak S, Kosicek M, Mladenovic-Djordjevic A, Smiljanic K, Kanazir S, Hecimovic S. Loss of cathepsin B and L leads to lysosomal dysfunction, NPC-like cholesterol sequestration and accumulation of the key Alzheimer's proteins. PLoS One 2016;11:e0167428.
38) Benhamouche S, Decaens T, Godard C, Chambrey R, Rickman DS, Moinard C, et al. Apc tumor suppressor gene is the "zonation-keeper" of mouse liver. Dev Cell 2006;10:759-770.
39) Cheng X, Kim SY, Okamoto H, Xin Y, Yancopoulos GD, Murphy AJ, et al. Glucagon contributes to liver zonation. Proc Natl Acad Sci U S A 2018;115:E4111-E4119.
40) Kietzmann T. Metabolic zonation of the liver: the oxygen gradient revisited. Redox Biol 2017;11:622-630.
41) Kietzmann T. Liver zonation in health and disease: hypoxia and hypoxia-inducible transcription factors as concert masters. Int J Mol Sci 2019;20:2347.
42) Matz-Soja M, Hovhannisyan A, Gebhardt R. Hedgehog signalling pathway in adult liver: a major new player in hepatocyte metabolism and zonation? Med Hypotheses 2013;80:589-594.
43) Clevers H. Wnt/beta-catenin signaling in development and disease. Cell 2006;127:469-480.
44) MacDonald BT, Tamai K, He X. Wnt/beta-catenin signaling: components, mechanisms, and diseases. Dev Cell 2009;17:9-26.
45) Rochard L, Monica SD, Ling IT, Kong Y, Roberson S, Harland R, et al. Roles of Wnt pathway genes wls, wnt9a, wnt5b, frzb and gpc4 in regulating convergent-extension during zebrafish palate morphogenesis. Development 2016;143:2541-2547.
46) **Yan Y**, **Jiang K**, Liu P, Zhang X, Dong X, Gao J, et al. Bafilomycin A1 induces caspase-independent cell death in hepatocellular carcinoma cells via targeting of autophagy and MAPK pathways. Sci Rep 2016;6:37052.
47) Forgac M. A new twist to V-ATPases and cancer. Oncotarget 2018;9:31793-31794.
48) Kulshrestha A, Katara GK, Ibrahim SA, Riehl V, Sahoo M, Dolan J, et al. Targeting V-ATPase isoform restores cisplatin activity in resistant ovarian cancer: inhibition of autophagy, endosome function, and ERK/MEK Pathway. J Oncol 2019;2019:2343876.
49) Whitton B, Okamoto H, Packham G, Crabb SJ. Vacuolar ATPase as a potential therapeutic target and mediator of treatment resistance in cancer. Cancer Med 2018;7:3800-3811.
50) Michel V, Licon-Munoz Y, Trujillo K, Bisoffi M, Parra KJ. Inhibitors of vacuolar ATPase proton pumps inhibit human prostate cancer cell invasion and prostate-specific antigen expression and secretion. Int J Cancer 2013;132:E1-E10.
51) Sudhan DR, Siemann DW. Cathepsin L targeting in cancer treatment. Pharmacol Ther 2015;155:105-116.
52) Aggarwal N, Sloane BF. Cathepsin B: multiple roles in cancer. Proteomics Clin Appl 2014;8:427-437.

Author names in bold designate shared co-first authorship.

Supporting Information

Additional Supporting Information may be found at onlinelibrary.wiley.com/doi/10.1002/hep.31305/suppinfo.